Supporting Information for

"Resolving Mixtures in Solution by Single-Molecule Rotational Diffusivity"

*Hsiang-Yu Yang and W. E. Moerner**

Department of Chemistry, Stanford University, Stanford, California 94305, United States

Contents

1. Correcting for high NA depolarization effects for different values of the collection half angle α

We first define the following transformation coefficients Q_0 and Q_2 following Fisz:[1]

$$Q_0 = \frac{1}{2}\frac{\cos\alpha - \cos^3\alpha}{1-\cos\alpha} \tag{S1}$$

$$Q_2 = \frac{1}{12}\frac{7 - 3\cos\alpha - 3\cos^2\alpha - \cos^3\alpha}{1-\cos\alpha} \tag{S2}$$

The magic angle for collection half angle α can then be expressed as

$$\theta_{mag}(\alpha) = \frac{1}{2}\cos^{-1}\left(-\frac{Q_0}{3Q_2}\right) \tag{S3}$$

We then define the following correction factors to account for high NA depolarization for both the time-resolved and steady-state anisotropy values:

$$c_r(\alpha) = Q_2 \tag{S4}$$

$$c_{tot}(\alpha) = \frac{1}{5}(Q_0 - Q_2) \tag{S5}$$

The correction for time-resolved anisotropy then becomes (main text eq 7):

$$r(t;\alpha) = c_r(\alpha) r_0 \exp(-t/\theta)$$

Here r_0 has a maximum value of 0.4 regardless of α.

In traditional experiments using a low divergence (nearly parallel) beam of light, the steady-state anisotropy is defined as

$$\bar{r_p} = \frac{\overline{I_\parallel} - \overline{I_\perp}}{\overline{I_\parallel} + 2\overline{I_\perp}} \tag{S6}$$

where $\overline{I_{\parallel}}$ and $\overline{I_{\perp}}$ correspond to the fluorescence brightness levels in our measurement. To remove the high NA effect and obtain a consistent value for different choices of objective and immersion oil, the steady-state anisotropy $\bar{r}$ can be calculated by

$$\bar{r} = \frac{\bar{r}_p}{c_r(\alpha) - 2.5c_{tot}(\alpha)\bar{r}_p} \tag{S7}$$

2. Control experiment: Maximum likelihood estimates of τ, θ, and r_0 for free Cy5 molecules

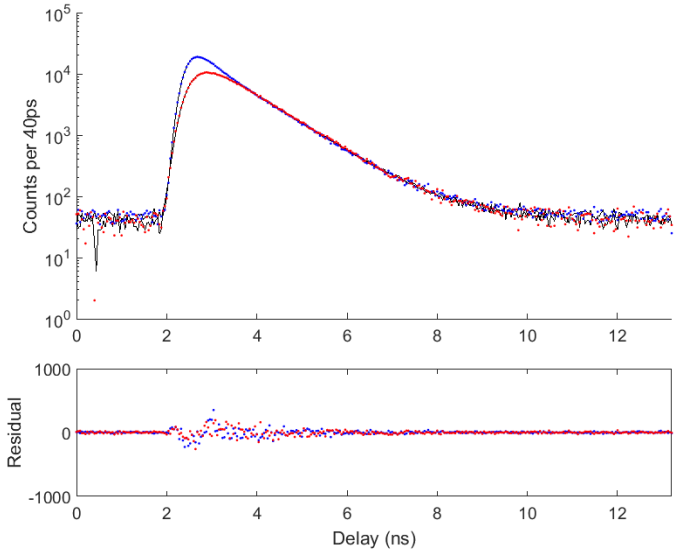

Figure S1. Top: A pair of TCSPC histograms for a bulk sample of 10 nM Cy5 in pure water (parallel channel in blue dots and perpendicular channel in red dots). The MLE model for each channel is shown by the solid black curves, with the MLE estimates τ = 0.919 ± 0.001 ns, θ = 0.40 ± 0.01 ns, and r_0 = 0.422 ± 0.01. While these measurements show high statistical precision from the fit, the accuracy would be expected to suffer a bit due to the fast dynamics compared to our relatively broad IRF. The rotational correlation time is one order of magnitude smaller than that of iCy5-labeled DNA, which is strongly immobilized by the attachment to DNA at both ends of Cy5. Bottom: Unweighted residuals.

3. DNA sequence design and dissociation rate estimate

The binding energy of the iCy5 labeled ssDNA and the unlabeled strand was estimated using the binding energy of the following two DNA oligomers with one mismatch:

5'-GGAGGACTGCGC-3' and 5'-GCGCACTCCTCC-3'

The estimated binding energy is 9.9 kcal/mol, calculated using the DINAMelt web server.[2] The corresponding dimensionless equilibrium constant for hybridization is $K_{eq} = 1.8 \times 10^7$.

For DNA oligomers, the binding rate constant is ~1 $\mu M^{-1} s^{-1}$ (see Supporting Information for ref 3). Therefore, the dissociation rate is estimated to be ~0.01 s^{-1}. The 100 s dissociation time is consistent with the fact that dissociations were seldom observed during the ~1 s observation times.

4. Instrument response function (IRF) measurement

In previous ABEL trap experiments with pulsed excitation for fluorescence lifetime measurements, the instrument response function was often measured by weak reflection of excitation laser, without the use of emission filters. This approach can cause systematic errors in the maximum likelihood estimate of rotational parameters, and the fluorescence-based IRF measurement described in the main text reduces this error by 75%.

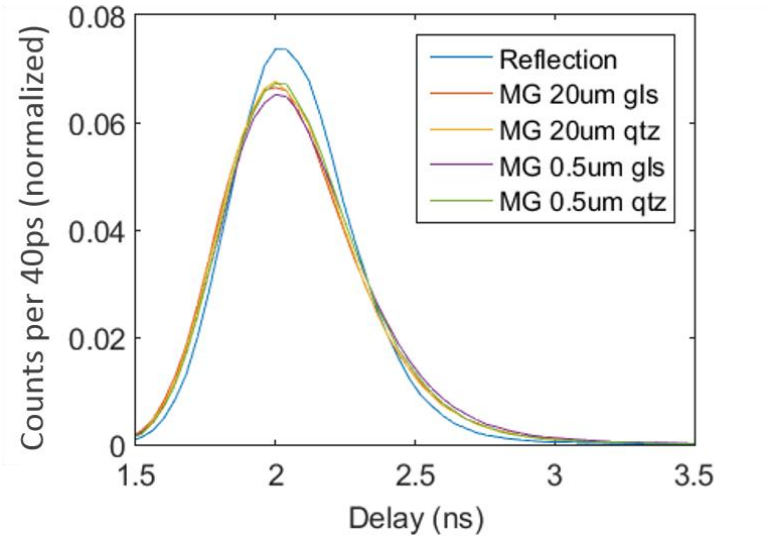

Figure S2. Instrument response function measured with reflection of the pumping light compared to the very short burst of fluorescence from malachite green (fluorescence lifetime ~1 ps). The fluorescence measurements were conducted with different coverslip materials, glass (gls) and quartz (qtz), and at different focal depth (0.5 or 20 μm above the coverslip/solution interface). The result shows that the fluorescence-based IRFs are relatively consistent but deviate from the reflection-based IRF.

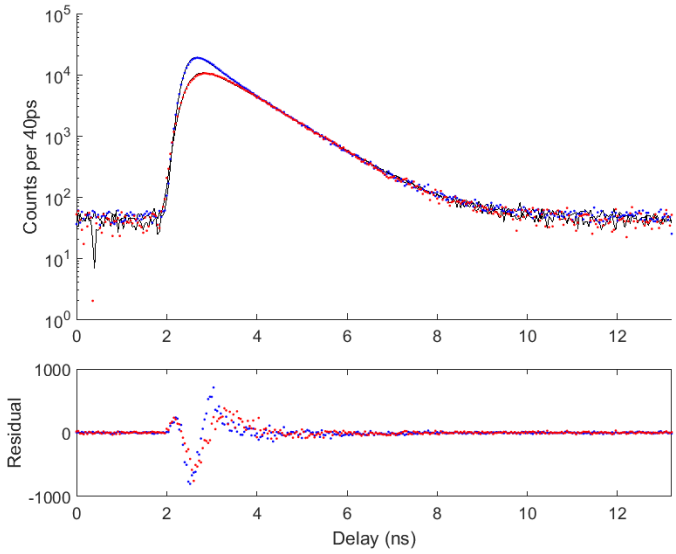

Figure S3. MLE fitting of bulk dsDNA fluorescence using reflection-based IRF yields high systematic errors in the residuals. Plots and fits with same color scheme as in Figure S1.

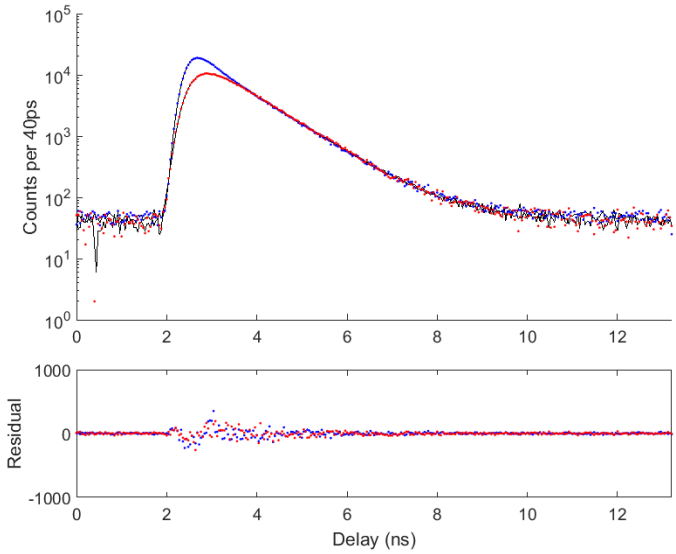

Figure S4. MLE fitting of bulk dsDNA fluorescence using fluorescence-based IRF reduces the amplitude of the systematic error by 75%. Plots and fits with same color scheme as in Figure S1.

5. Control experiment: Anisotropy of bulk ssDNA and dsDNA samples using collimated laser excitation and low NA detection optics

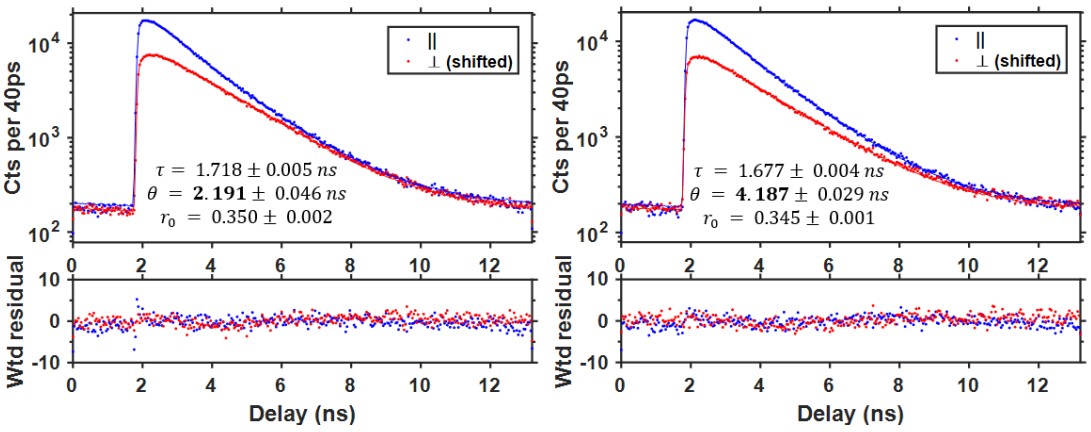

Figure S5. Bulk ssDNA and dsDNA measurements of anisotropy parameters using collimated laser excitation and low NA detection optics, data analyzed on a photo-by-photon basis as in the single-molecule measurements. Left: 1 μM ssDNA. Right: 1 μM dsDNA (1 μM ssDNA with 5 μM unlabeled complement).

6. Modeling the shift of instrument response function

The response of the APD detectors can be slightly different for different wavelengths of incident light. This effect is known as "color shift".[4] To account for the different emission wavelengths of malachite green and iCy5, as well as other sources of IRF shift during experiments, we explicitly model the IRF shift in our probability function. Our MLE procedure takes two IRF shifts $c_{\parallel}$ and $c_{\perp}$ (for parallel and perpendicular channels, respectively) as fitting parameters. Each channel is treated independently.

The pulse-photon delays in our TCSPC experiments are grouped into 40 ps bins. To model the IRF shifts using a higher time resolution, we use a two-step process. First, given a trial color shift $c_{\parallel}$ (or $c_{\perp}$; here we use the parallel channel as an example), we calculate floor($c_{\parallel}$) and ceil($c_{\parallel}$), the two closest bins. Then we shift the measured IRF in the 13.2 ns window (corresponding to 76 MHz repetition rate), cyclically, using either floor($c_{\parallel}$) or ceil($c_{\parallel}$). Second, the two shifted IRFs are weighted properly and summed together to generate the final shifted IRF:

$$\mathrm{IRF}_{\parallel}(t; c_{\parallel}) = \left(1 - \frac{c_{\parallel} - \mathrm{floor}(c_{\parallel})}{40\ \mathrm{ps}}\right) * (\mathrm{IRF}_{\parallel} \text{ shifted using floor}(c_{\parallel})) + \left(\frac{c_{\parallel} - \mathrm{floor}(c_{\parallel})}{40\ \mathrm{ps}}\right) * (\mathrm{IRF}_{\parallel} \text{ shifted using ceil}(c_{\parallel})) \quad \text{(S8)}$$

7. Difference between the ssDNA and dsDNA $p(\bar{r}, \theta)$ used in dsDNA/ssDNA classification analysis

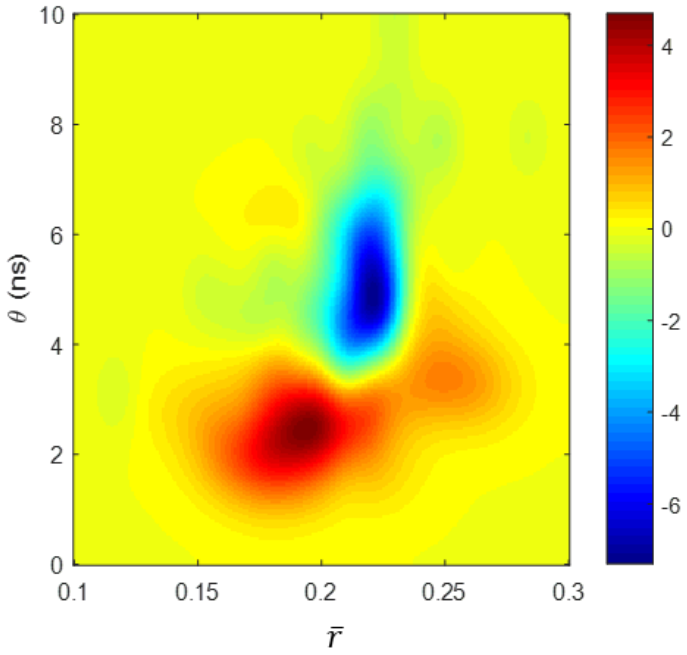

Figure S6. The difference between the ssDNA and dsDNA $p(\bar{r}, \theta)$ distributions.

8. Estimation of reorientation energy due to Debye layer

The maximum electric field in our ABEL trap experiments is on the order of 1 V/μm at the feedback gains needed for trapping. One may ask if this causes a distortion of the rotational dynamics, especially for the dsDNA. Here we show that the estimated reorientation energy for trapped dsDNA oligomers (likely also valid for many other common biomolecules) in this electric field is much smaller than thermal energy k_BT. Therefore, this effect is negligible and the trapped molecules still freely rotate.

First of all, the permanent dipoles of DNA oligomers are very small, and the small size of DNA oligomers makes the polarizability anisotropy also very small (compared to objects like gold nanorods). A larger contribution may arise from the field-induced redistribution of counter ions in solution. For example, in a study of negatively charged gold nanorods,[5] $\Delta\alpha$, the difference between the longitudinal and transverse polarizabilities, was measured to be ~10^{-32} Fm^2, but this value is 30 times higher than expected from gold alone and is primarily due to the polarizable Debye layer. Using scaling based on the surface area for objects with similar aspect ratio in ref 5, we may estimate $\Delta\alpha$ for our dsDNA to be ~10^{-34} Fm^2. The reorientation energy $(\Delta\alpha)E^2$, is two orders of magnitude smaller than k_BT, where E is the electric field strength.

Even in a worst-case hypothetical scenario, where all counter ions move to one half of a dsDNA molecule when the electric field is applied, the induced dipole moment is estimated to be ~3.6×10^{-27} Cm for parallel aligned dsDNA, and ~1.9×10^{-27} Cm for perpendicularly aligned dsDNA. The reorientation energy in this case is 1.7×10^{-21} J, still significantly lower than the thermal energy. It is worth noting that this worst-case scenario is very unlikely to happen, as the feedback electric field is much smaller compared to the electric fields around or within biomolecules.

9. Absorption spectra of internally labeled DNA oligomers

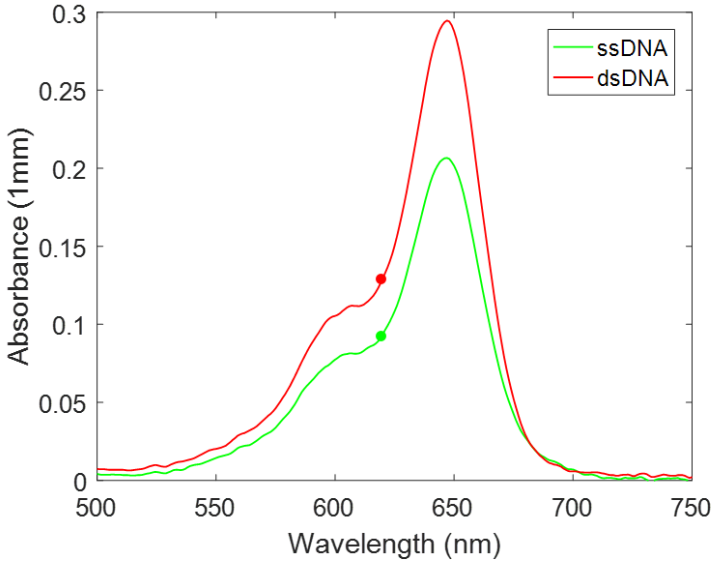

Figure S7. Absorption spectra of 10 μM ssDNA (green curve, with no unlabeled strand) and 10 μM dsDNA (red curve, with 50 μM unlabeled strand). Absorbance (1 mm) at 620 nm is 0.095 for ssDNA (green dot) and 0.13 for dsDNA (red dot).

10. Time duration of constant brightness ("level") distribution

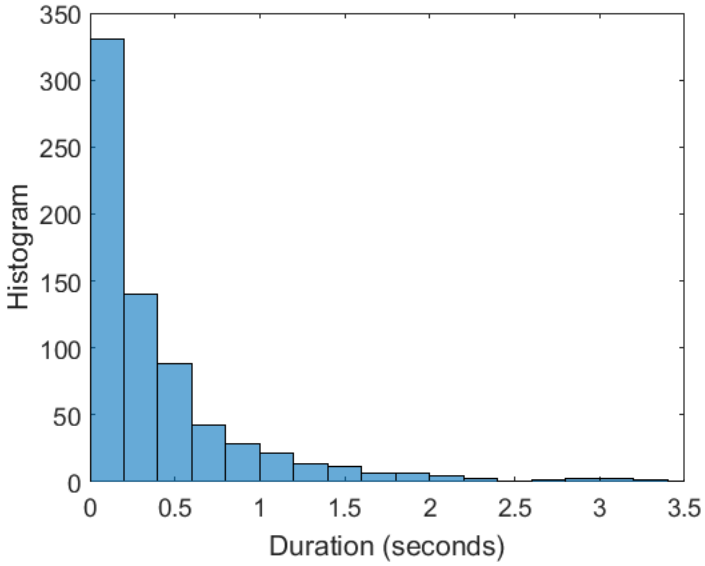

Figure S8. Distribution of time duration of constant brightness ("level") in a typical dsDNA trapping experiment.

References

(1) Fisz, J. J. *J. Phys. Chem. A* **2007**, *111*, 8606-8621.

(2) Markham, N. R.; Zuker, M. *Nucleic Acids Res.* **2005**, *33*, 577-581.

(3) Wang, Q.; Moerner, W. E. *Nat. Methods* **2014**, *11*, 555-558.

(4) *Advanced Photon Counting: Applications, Methods, Instrumentation*; Kapusta, P., Wahl, M., Erdmann, R., Eds.; Springer Series on Fluorescence 15; Springer: 2015.

(5) Zijlstra, P.; van Stee, M.; Verhart, N.; Gu, Z.; Orrit, M. *Phys. Chem. Chem. Phys.* **2012**, *14*, 4584.